Journal of Science and Transport Technology
Journal homepage: https://jstt.vn/index.php/en

Comparative Study on the Probabilistic Safety of Truss Structures Designed Using U.S. and Vietnamese Codes

Nhu Son Doan[1,*], Anh Tuan Tran[2]
[1]Faculty of Civil Engineering, Vietnam Maritime University, 484 Lach Tray Street, Le Chan district, Haiphong 180000, Vietnam
[2]University of Transport Technology, 54 Trieu Khuc, Thanh Xuan, Hanoi 100000, Vietnam

Article info
Type of article:
Original research paper

DOI:
https://doi.org/10.58845/jstt.utt.2025.en.5.1.1-14

***Corresponding author:**
Email address:
vanson.ctt@vimaru.edu.vn

Received: 15/11/2024
Received in Revised Form: 19/12/2024
Accepted: 10/01/2025

Abstract: This study evaluates and compares the reliability of a truss designed according to the Vietnamese TCVN 5575-2012 and the American AISC 360-16 steel design codes. The same truss configuration and applied loads are considered, with sections designed according to each standard. Their probabilistic safety levels are then evaluated to provide deeper insights into the differences between the design codes. Results indicate that, under identical loading, trusses designed with AISC are lighter than those designed with TCVN, as TCVN requires larger sections for compression members. Reliability indexes (RIs) for tension behavior are similar between codes; however, TCVN yields higher RIs for buckling, indicating a conservative approach for compression members compared to AISC. Although TCVN does not specify a target RI, its deterministic and probabilistic safety levels exceed those of AISC, suggesting a target RI above AISC's 3.0. Consequently, TCVN-based designs generally involve higher costs, emphasizing the importance of understanding safety implications in code selection. Finally, the conservative results from TCVN are examined through equivalent safety factors, providing insights into its design assumptions.

Keywords: Truss structure; Reliability analysis; Monte-Carlo simulation; FEM; Probabilistic safety; Fully probabilistic analysis.

1. Introduction

In 2023, TCVN 2737-2020 underwent a tentative update from its previous version, TCVN 2737-1995, marking a significant transition from the allowable stress design (ASD) approach to a limit state design framework. An additional revision, TCVN 2737-2023, has been proposed to further enhance this transition. This shift is important, as load and resistance factors (LRFs) derived from reliability-based methods improve uniformity and consistency in design [1-4]. Reliability-based design codes are widely adopted in North America, Europe, and Japan [4]. These codes apply load factors to manage uncertainties in load effects and resistance factors to account for material capacity uncertainties, both determined through probabilistic analysis. Furthermore, the limit state design process is similar to ASD, making it readily accessible to design engineers without extensive training in reliability calculations.

Historically, limit state design codes were developed to offer a more accessible design approach for engineers with limited knowledge of probabilistic analysis while also accounting for real-world uncertainties. Reliability-based methods are employed to calibrate the load and resistance factors during the development of these codes. The load factors, defined in the "load and actions codes" (e.g., ASCE/SEI 7-16 [5]), and the resistance factors, specified in design codes for various materials such as steel and concrete, must be calibrated to achieve the target reliability index (RI). This ensures that design solutions using limit state codes are intended to provide consistent safety levels from a probabilistic perspective. For example, target reliability indexes of 3.0 and 3.8 are specified for steel structures designed using AISC 360-16 [6] and EC3 [7], respectively.

Since the uncertain models of loads are not recommended in the new version of TCVN 2737, and the target reliability index is not defined in the steel design code of TCVN 5575-2012 [8], the probabilistic safety level of the design solutions obtained from TCVN codes becomes questionable. Consequently, the cost investment may become expensive if the safety is highly set. In addition, the steel design code of TCVN 5575-2012 was developed for the load evaluated following the old version of the load and actions code (i.e., TCVN 2737-1995). Thus, the steel sections designed following the steel design code and using the load effects estimated from the TCVN 2737-2020 need to be investigated.

Because the 2023 version of TCVN 2737 retains the same load factors as the original TCVN 2737-1995, this study evaluates the consistency of the load factors and combinations proposed in TCVN 2737-2020, along with the factors influencing the capacity of steel elements specified in TCVN 5575-2012. For comparison, the American design codes ASCE/SEI 7-16 [5] and AISC 360-16 [6] are also used as references. These comparisons offer valuable insights into the reliability levels of the Vietnamese codes. Accordingly, the truss sections are initially designed according to both design codes, as detailed in Section 2. The failure probability and reliability indexes of the design solutions are then evaluated using Monte Carlo simulations (MCS), as described in Section 3. An illustrative example of the truss structure is provided in Section 4, followed by the results and discussion. The study concludes in Section 5.

2. Limit state designs of truss structures following AISC 360-16 and TCVN

Hereafter, the codes ASCE/SEI 7-16 and AISC 360-16 are collectively referred to as AISC, and TCVN 2737-2020 and TCVN 5575-2012 as TCVN. The truss design process for both approaches is outlined in Fig. 1. Generally, axial forces in truss members are calculated based on applied loads, with resultant forces combined according to load and action code provisions. Tension and compression members are designed to adequately support the applied loads, with buckling conditions checked to ensure compact sections and maintain member resistance. Finally, deformations are evaluated to satisfy serviceability limits.

It should be noted that the “standard values of loads” are commonly specified in the TCVN 2737, depending on the members designed. For instance, the standard values of live load acting on floors of offices and departure lounges at airports are specified as 20 kPa and 40 kPa, respectively. On the other hand, the nominal terms are commonly used in ASCE/SEI 7 and AISC 360-16. While the nominal values in AISC and standard values in TCVN are both unfactored quantities and thus interchangeable, the dead and live load inputs must be adjusted to yield equivalent factored loads in both design processes for accurate comparison. For simplicity, this study adopts nominal terms.

The two design codes of ASCE/SEI 7-16 and TCVN 2737-2020 are based on the limit state design approach. The strength limit state is focused on in this work. Only two actions of dead and live loads are examined; hence, the factored loads following ASCE/SEI 7-16 and TCVN 2737-2020 can be presented in Eqs. (1) and (2), respectively. In the equations, D_n and L_n represent the nominal resultants caused by dead and live loads, respectively. Equations indicate that if the same nominal loads are applied, the combination effects differ between the two design codes. Conversely, to achieve the same factored load, different nominal loads must be applied for each design code. The resultants in the equations correspond to the tension or compression forces within the truss members. The FEM-Truss program, developed in MATLAB [9], is employed to assess the axial forces.

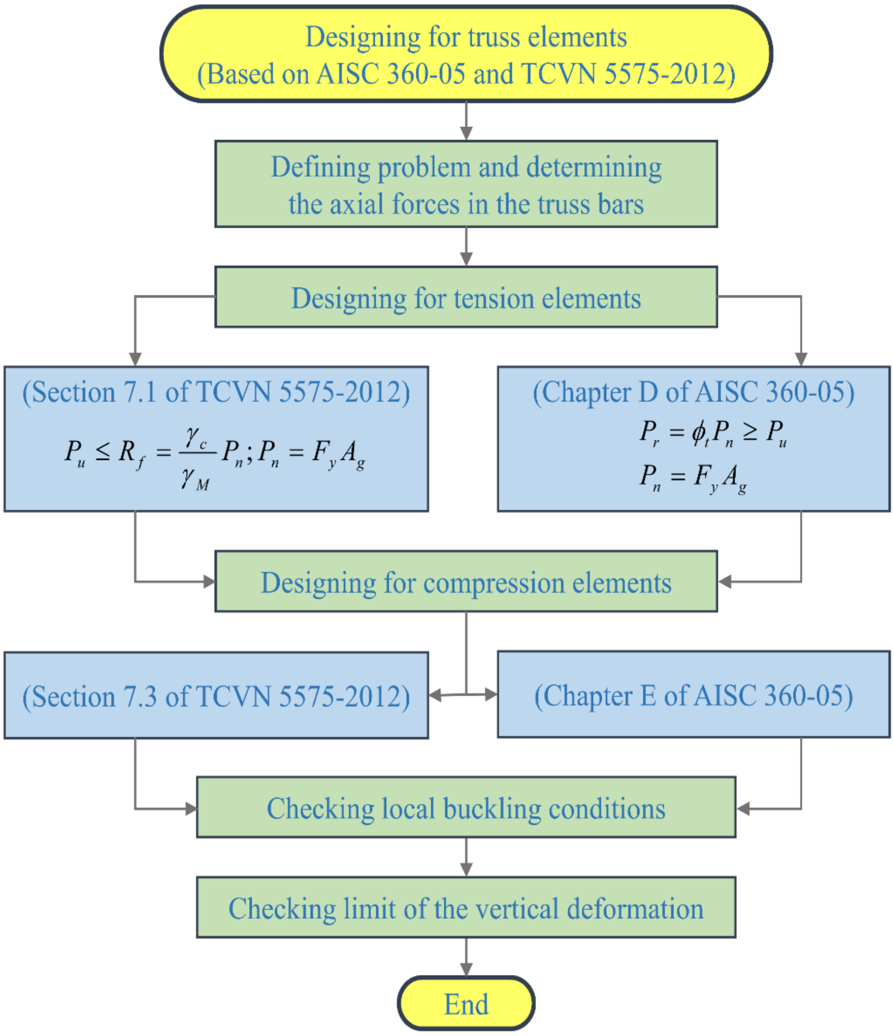

Fig. 1. Flowchart for designing truss members

$$P_u^{VN} = 1.35D_n + 1.50L_n \quad (1)$$

$$P_u^{AC} = 1.20D_n + 1.60L_n \quad (2)$$

The sections of the tension elements are then designed to withstand the axial loads calculated. Noticeably, the stress checking is performed following TCVN as shown in Eq. (3). In Eq. (3), N is factored load, i.e., P_u^{VN} in Eq. (1), A_g is the gross area of sections. γ_c is the factor of working condition, and *f* is calculated stress. On the other hand, AISC used the LRFD format for force checking in the design practice, as shown in Eq. (4). In Eq. (4), P_u (similar role as N in Eq. (3)) is the load effects combined from Eq. (2). P_r is the factored resistance for tensions.

$$N/A_g \le \gamma_c f \quad (3)$$

$$P_u \le P_r = \phi P_n \quad (4)$$

To facilitate comparison, the LRFD format is used for the design processes according to both design codes. Thus, the design equation of TCVN is converted to the form of LRFD, as presented in Eq. (5). Noteworthy, the calculated stress (f) is determined from yield stress (i.e., f_y in TCVN and F_y in AISC) considering the partial factor for material property (γ_M), as shown in Eq. (6). Therefore, the factored resistance P_r is calculated by taking into account both the partial safety factor for material property and for the working condition (γ_c), as shown in Eq. (5).

$$N = P_u^{VN} \le P_r$$
$$\text{where } P_r = \gamma_c\left(fA_g\right) = \frac{\gamma_c}{\gamma_M}\left(f_y A_g\right) = \frac{\gamma_c}{\gamma_M}P_n \quad (5)$$

$$f = f_y/\gamma_M = F_y/\gamma_M \quad (6)$$

Similarly, the design equation for the compression bars relating to the buckling condition in TCVN is converted from the original equation (Eq. (7)) to the LRFD format as Eq. (8). In the equations, φ is the buckling factor. The design process using the two design codes is summarized in Fig. 1, while Fig. 2 outlines the design procedure for compression bars. In the figures, F_{cr} is the critical stress, and F_e is the elastic buckling stress. λ and $\bar{\lambda}$ are the slenderness and nominal slenderness, respectively.

$$\frac{N}{\varphi A_g} \le f\gamma_c \quad (7)$$

$$N = P_u^{VN} \le P_r = \frac{\gamma_c}{\gamma_M}\left(\varphi f_y A_g\right) = \frac{\gamma_c}{\gamma_M}P_{cr} \quad (8)$$

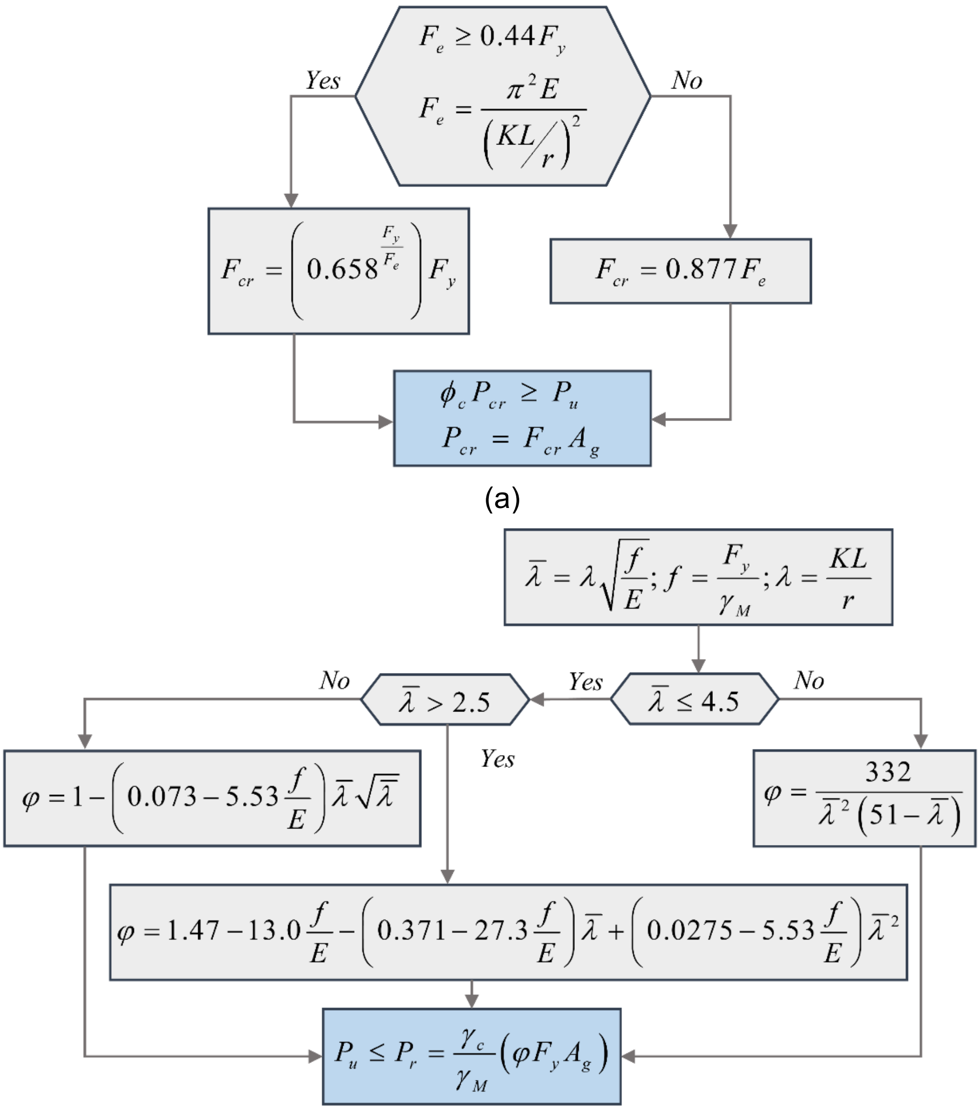

Fig. 2. Designing flowcharts for compression members: (a) using AISC 360-16; (b) using TCVN 5575-2012

For the designs using TCVN 5575-2012, the partial factor for material property (γ_M) is taken as 1.10, as recommended in Section 6 of the standard. The factors of working conditions are specified as 0.95 and 0.90 for designing tension and compression bars, respectively. Regarding AISC 360-16, the LRFD format is applied directly, using resistance factors of 0.90 for both tension (ϕ_t) and compression (ϕ_c) members, as specified in Chapters D and E of the code.

Finally, the width-to-thickness ratios of compression bars are evaluated to guarantee compact sections and mitigate the risk of local buckling. For the box sections, the limiting width-to-thickness ratio is given in Table B4.1 of AISC and shown in Eq. (9) below. For TCVN, the limiting values are specified in Table 33 of the standard, as outlined in Eq. (10) below. Moreover, the slenderness ratio limits (200 for compression members and 300 for tension members) must also be verified using the effective lengths of the components. An effective length factor of 0.9 is chosen for the compression members [10,11].

$$\frac{b_w}{t_w} \le 1.4\sqrt{\frac{E}{F_y}f} \tag{9}$$

$$\begin{aligned} &\frac{b_w}{t_w} \le 1.2\sqrt{\frac{E}{F_y}} && \text{if } \bar{\lambda} < 1 \\ &\frac{b_w}{t_w} \le \left(1+0.2\bar{\lambda}\right)\sqrt{\frac{E}{F_y}} \le 1.6\sqrt{\frac{E}{F_y}} && \text{if } \bar{\lambda} \ge 1 \end{aligned} \tag{10}$$

3. Fully probabilistic analysis for truss structures

The methods of reliability analysis have been thoroughly discussed in the literature., e.g., [3,12]. Three distinct reliability analysis methods were used to assess the sliding stability of caisson breakwaters [13]. Monte Carlo simulation is a simple yet effective method that not only provides the failure probability but also offers statistical insights into the performance functions. Particularly for nonlinear and high-dimensional problems, MCS proves to be the most suitable approach, making it superior to other methods [4]. The primary disadvantage of MCS is the considerable computational time and effort it demands, as it requires a large number of calculations [14,15]. Recent advancements in computing have greatly improved the efficiency of integrating MCS with FEM.

The MCS-based reliability analysis applied to the truss structure was presented in our previous works [9,14]. The main steps are summarized as follows.

Step 1. Defining the truss problem.

In this step, the deterministic and uncertain variables will be defined. In this analysis, the truss profile and boundary conditions are considered deterministic, while the uncertainty variables, sourced from previous studies on AISC 360-16, are summarized in Table 1 [2,5]. Moreover, uncertainties relating to the steel sections and material properties are taken from previous studies [6,10].

Table 1. Considered uncertainties

No.	Symbol	Description	Unit	μ	COV	Distribution
1	t_c	Thickness of comp. bars	mm^2	0.964	0.04	Normal
2	t_t	Thickness of tension bars	mm^2	0.964	0.04	Normal
3	t_w	Thickness of web members	mm^2	0.964	0.04	Normal
4	E	Young's modulus	GPa	1.00	0.06	Normal
5	F_y	Yield strength	MPa	1.10	0.10	Normal
6	D	Dead load	kN	1.05	0.10	Normal
7	L	Live load	kN	1.00	0.25	Extreme type 1

Step 2. Using MCS to create a set of input variables corresponding to the statistics defined in Step 1.

Step 3. Determining the axial forces in the truss bars using the *FEM-Truss* program developed in MATLAB [9].

Step 4. Evaluating resistances associated with each sampling set in the MCS. The tension and compression capacities are calculated as presented in Section 2.

Step 5. Assessing the performance functions for each sampling set. The performance function can be defined in Eq. (11). In Eq. (11), *R* denotes the resistance, and *Q* denotes the load. Noticeably, Eq. (11) can be used for both tension and compression bars.

$$g = R - Q \tag{11}$$

Step 6. Determining the failure probability and reliability index. The failure probability (P_f) in MCS is determined as the ratio of the number of failure events (N^{fails}) and the total number of simulations (N_{MCS}) using Eq. (12). The reasonable size for MCS was investigated in previous works [9]. For trusses designed at limit states, the MCS size of 1 million can be used [9]. Then, the reliability index β is approximated using Eq. (13), wherein Φ is the standard normal distribution.

$$P_f = N^{fail}/N_{MCS} \tag{12}$$

$$\beta = \Phi^{-1}\left(1 - P_f\right) \tag{13}$$

4. Illustrative examples

A truss profile shown in Fig. 3(a) is examined. This truss was investigated in previous works [9,10,15]. Since the load factors are different in the two design codes, the same factored load of 130 kN is used in this study. The nominal values of dead load (D) and live load (L) are then determined based on a ratio of live load to dead load of 3.0. Using the FEM-Truss, the same factored axial forces using TCVN and AISC are determined, as shown in Fig. 3(b). The square hollow section of 120 × 120 × 5.6 mm is kept the same as designed in the previous work for web members [10].

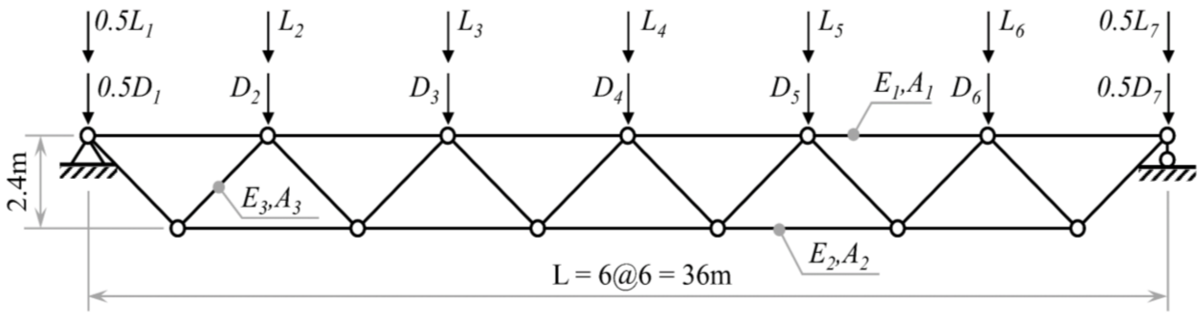

(a)

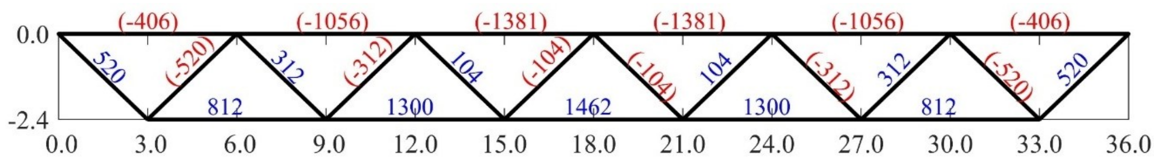

(b)

Fig. 3. Example of Waren truss: (a) Truss profile; (b) Axial forces obtained from load combinations of 1.2D+1.6L in ASCE/SEI 7-16 and 1.35D+1.50L in TCVN 2737-2020

4.1. Limit state design of the chord members

The design of the lower and upper chord members is carried out using both design codes, as presented in Section 2. Square hollow sections given by the SSAB Domex Tube (available at www.ssab.com) are used for the design processes. The steel material is characterized by a yield strength of 350 MPa and Young's modulus of 200

GPa. Given the differences in load and resistance factors between the two design codes, the unity value of the ratio P_r/P_u is established to identify the design solutions that satisfy the “limit state” criteria for each code. The feasible solutions indicated by the circle markers in Figs. 4 and 5 correspond to compression and tension members. The dashed lines in Figs. 4 and 5 represent the exact limit state designs for both design codes.

The width-to-thickness ratios governing the local bucking of the section are summarized in Fig. 6(a) for AISC and Fig. 6(b) for TCVN, respectively. Finally, the global buckling conditions are summarized in Fig. 7.

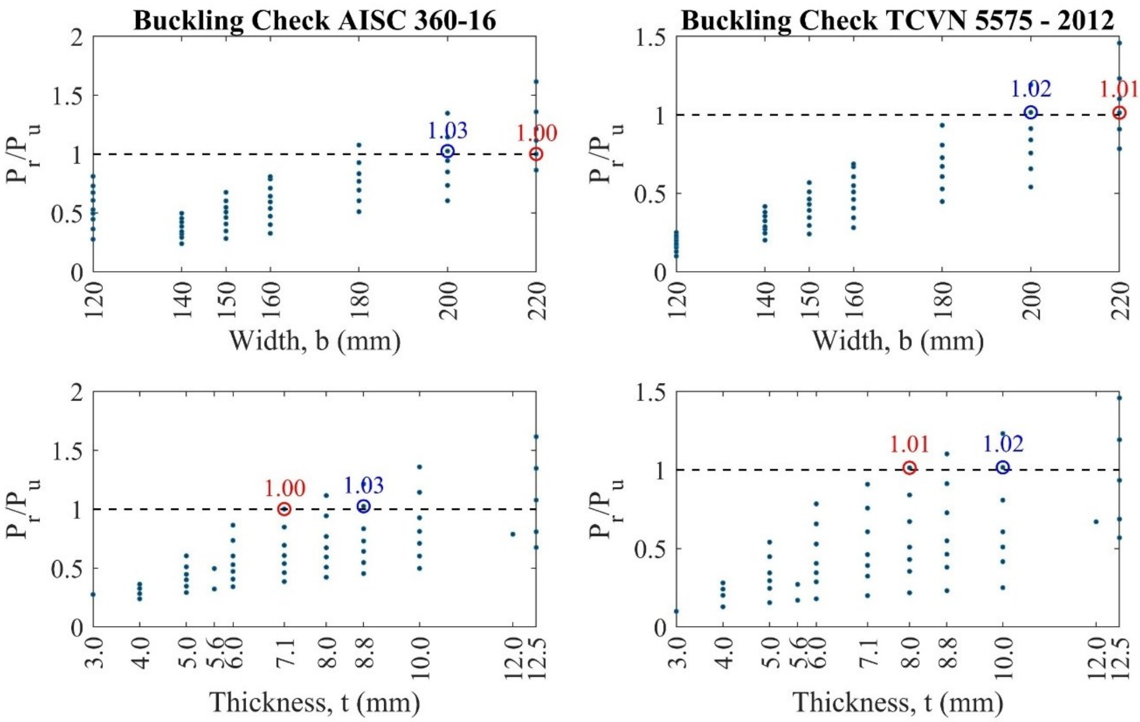

Fig. 4. Strength assessment of compression members

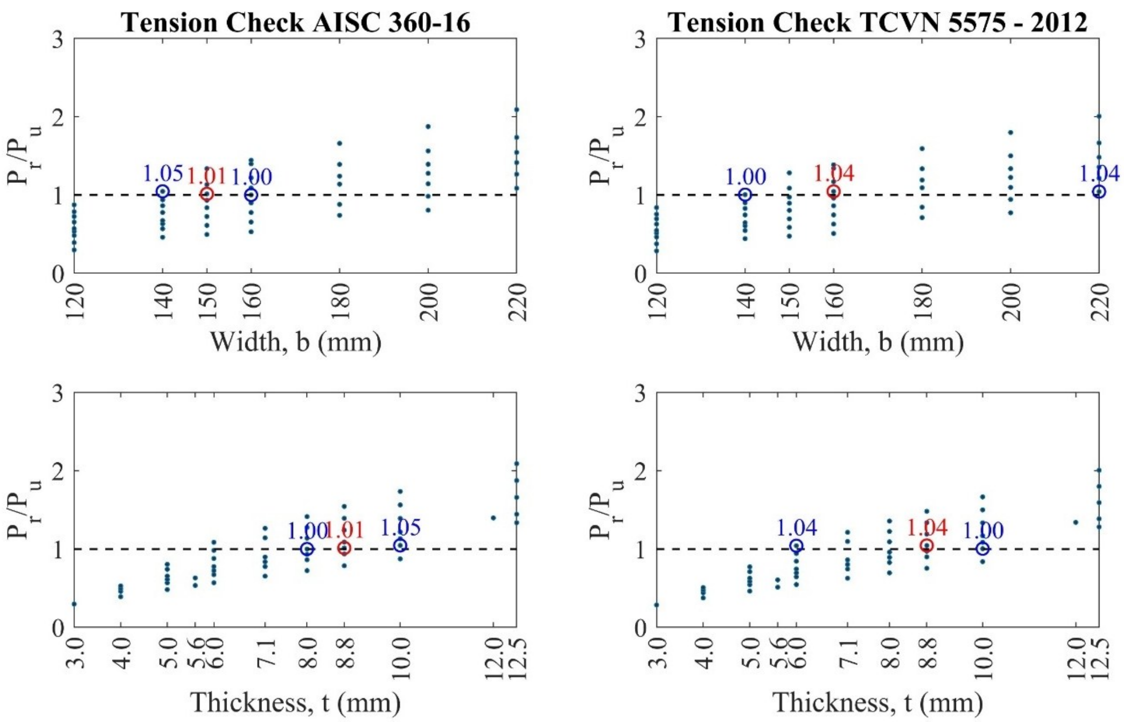

Fig. 5. Strength assessment of tension members

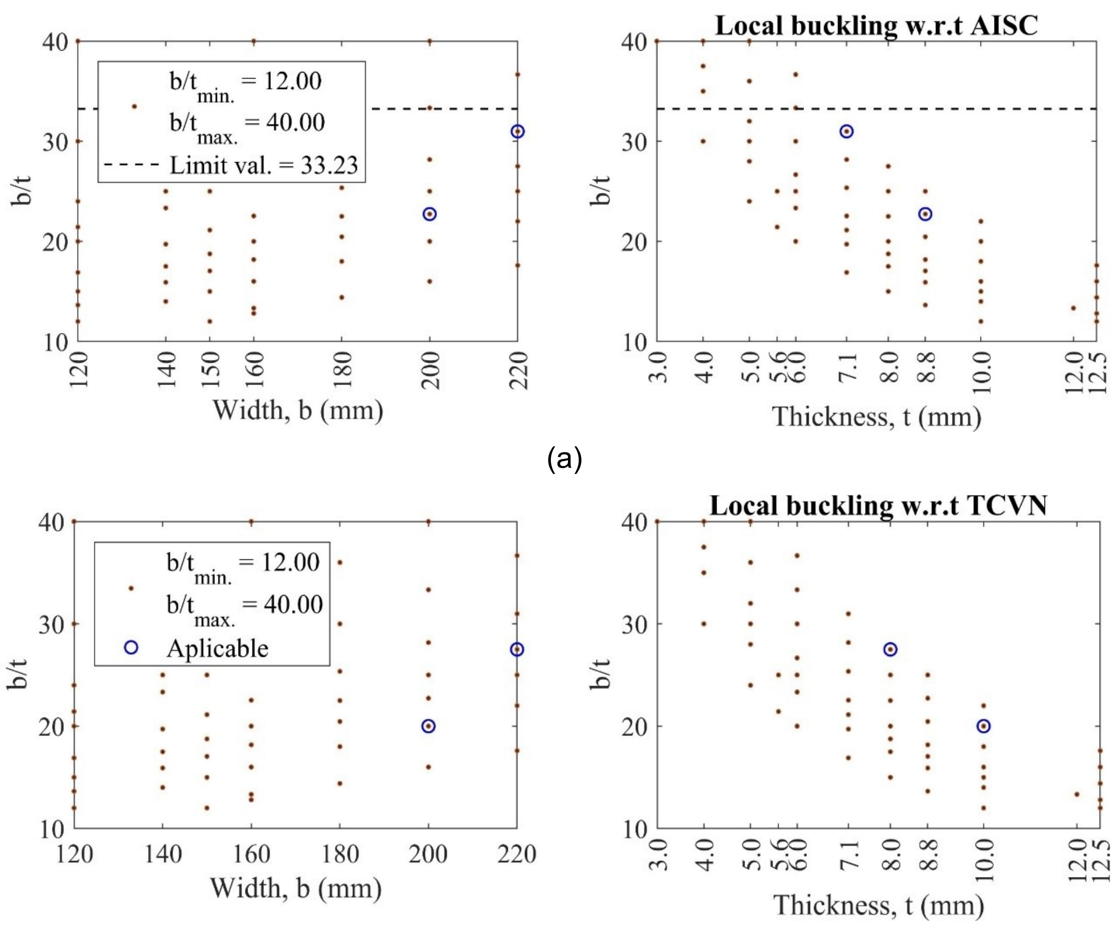

Fig. 6. Local buckling check for compression sections: (a) following AISC; (b) following TCVN

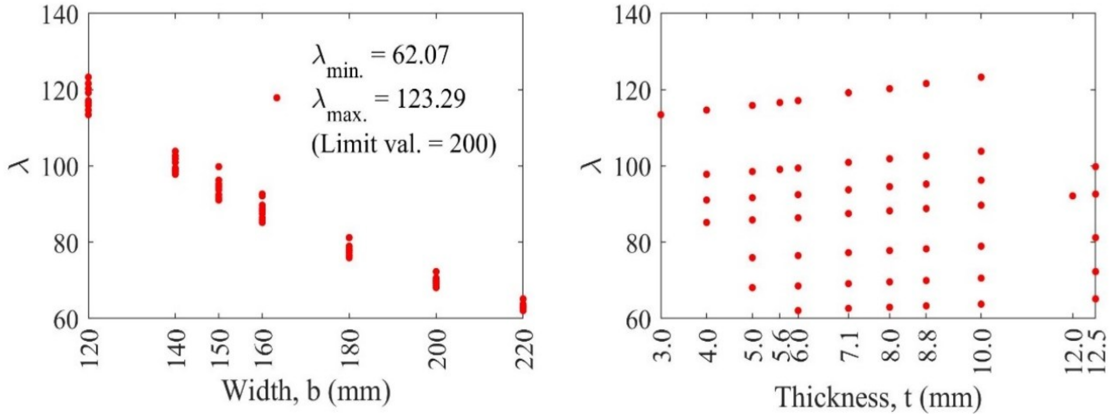

Fig. 7. Global buckling checking of chord bars $(\lambda = KL/r)$

Table 2. Comparison of the suitable sections

No.	Behavior	Sections and (P_r/P_u)	
		Using AISC (mm)	Using TCVN (mm)
1	Tension	160 × 8 (1.00)	140 × 10 (1.00)
2	Tension	150 × 8.8 (1.01)	160 × 8.8 (1.04)
3	Tension	140 × 10 (1.05)	220 × 6 (1.04)
4	Compression	220 × 7.1 (1.00)	220 × 8 (1.01)
5	Compression	200 × 8.8 (1.03)	200 × 10 (1.02)

Based on the strength and buckling conditions reported in Figs. 4 to 7, the feasible sections for tension bars designed following TCVN are 140 × 10 mm, 160 × 8.8 mm, and 220 × 6 mm. For AISC, the feasible sections for tension bars are 140 × 10 mm, 150 × 8.8 mm, and 160 × 8 mm. For the compression members, the sections of 220 × 10 mm and 220 × 8 mm are collected following TCVN. Using AISC, the selected sections for compression are 200 × 8 mm and 220 × 7.1 mm. The collected sections are summarized in Table 2. The ratio between P_r and P_u for each design solution is also presented by values in parentheses in the table. Based on the limit state design, it can be concluded that larger sections are necessary for the design solutions following TCVN, even though the same factored axial forces are considered. The probabilistic analysis is performed for all sections listed in Table 2 and presented in Subsection 4.2.

4.2. Comparison of the probabilistic results

The MCS-based reliability analysis described in Section 3 is applied to all design solutions listed in Table 2. For illustration, the probabilistic results for tension behavior are shown in Figs. 8(a) and 8(b) for AISC and TCVN, respectively. Notably, the same section, 140 × 10 mm, is used in Fig. 8 for tension design with both codes. Comparisons of tension behavior between the two codes for this section are summarized in Fig. 9. Similarly, Fig. 10(a) presents the results for compression behavior using a 200 × 8.8 mm section designed with AISC, while Fig. 10(b) shows the MCS results for a 200 × 10 mm section designed with TCVN. A comparison of the MCS results for compression behavior between these two sections is provided in Fig. 11.

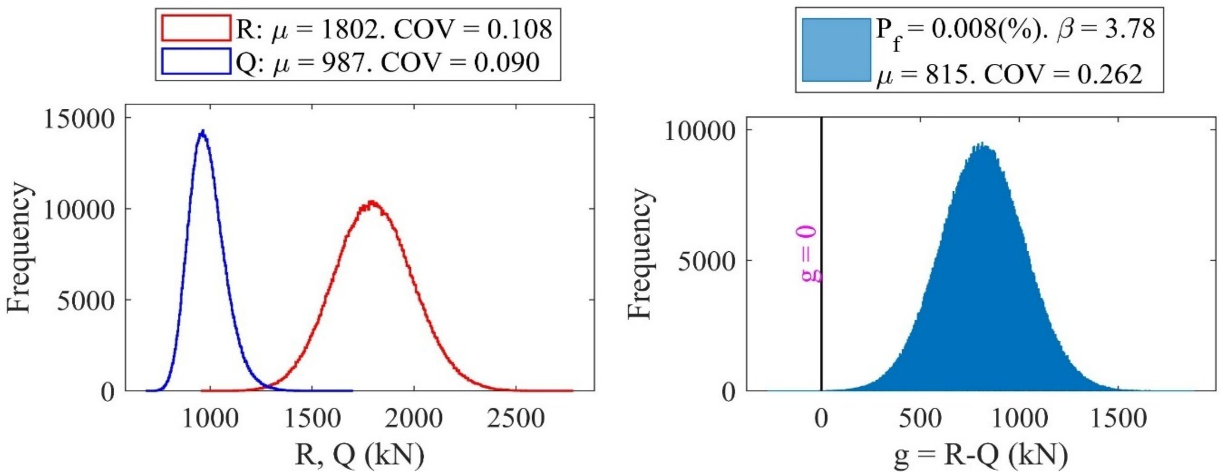

(a)

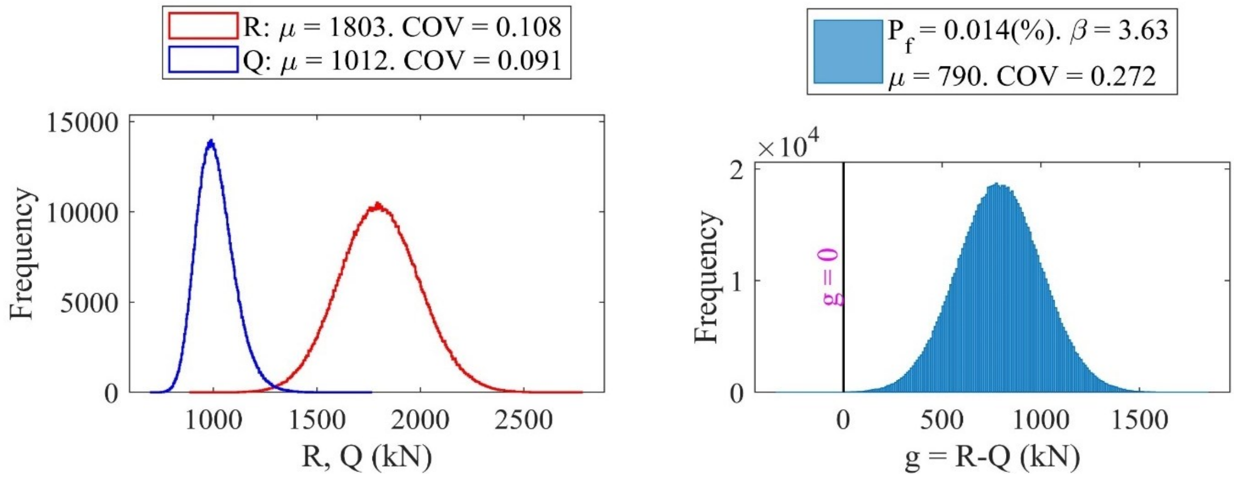

(b)

Fig. 8. Results of MCS for tension bars using section 140×10 mm: (a) Following AISC; (b) Following TCVN

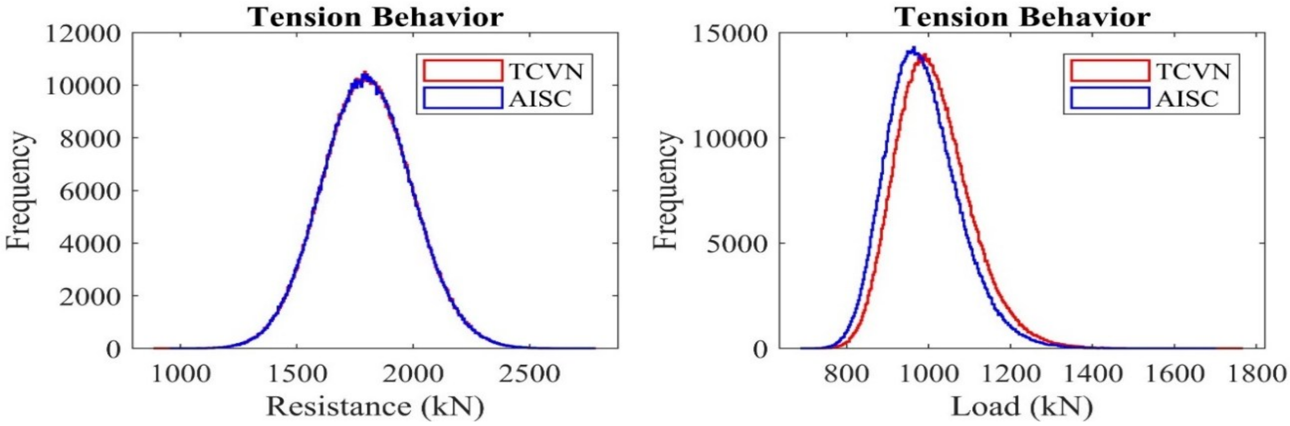

(a)

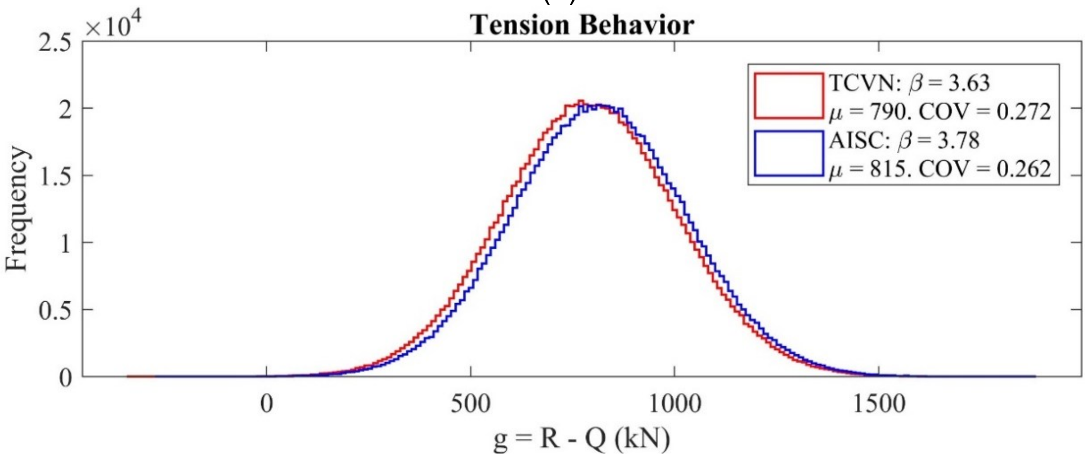

(b)

Fig. 9. Comparing results of tension behaviors

The left panels of Figs. 8 and 9 (a) reveal that the tension resistances are comparable for both codes, as the same section is used in the designs. However, the mean tension loads derived from TCVN 2737-2020 are approximately 2.5% higher than those from ASCE/SEI 7-16. Consequently, the reliability index (RI) for the TCVN-based design is slightly lower (3.63) than that for AISC (3.78), reflecting the inverse relationship between safety levels and applied loads. This observation suggests that the load factors specified in TCVN 2737-2020 may result in marginally higher load effects compared to ASCE/SEI 7-16.

Similarly, compression loads under TCVN are also approximately 2.5% higher, as shown in the left panels of Fig. 10. However, the larger section employed in the TCVN design results in a significantly higher resistance—about 11% greater in terms of the mean compression resistance compared to AISC. As a result, TCVN achieves a higher RI for compression behavior (4.53) than AISC (4.04). Notably, the coefficients of variation for both resistance and axial loads remain consistent across behaviors for both codes, indicating that the same level of uncertainty is considered in the comparisons. These findings highlight that the factors prescribed by the two design codes lead to notable differences in limit state designs and probabilistic safety outcomes.

Fig. 12 presents the reliability indexes for all analyzed sections under both tension and compression behaviors. It should be noted that the target RI of 3.0 is prescribed in AISC 360-16, but no value of target RI is recommended in TCVN. The figure indicates that for the same design code, the reliability index shows a positive relationship with the ratio of P_r/P_u.

Additionally, sections designed using TCVN consistently exhibit higher RIs compared to those designed with AISC, with the disparity being more pronounced for compression behavior, as highlighted in the right panel of Fig. 12. The limit state designs summarized in Table 2, combined with the probabilistic results presented in Fig. 12, clearly indicate that TCVN leads to more conservative design solutions. This reflects the conservative nature of the load and resistance factors defined in TCVN.

Further analysis of these findings is provided in Subsection 4.3.

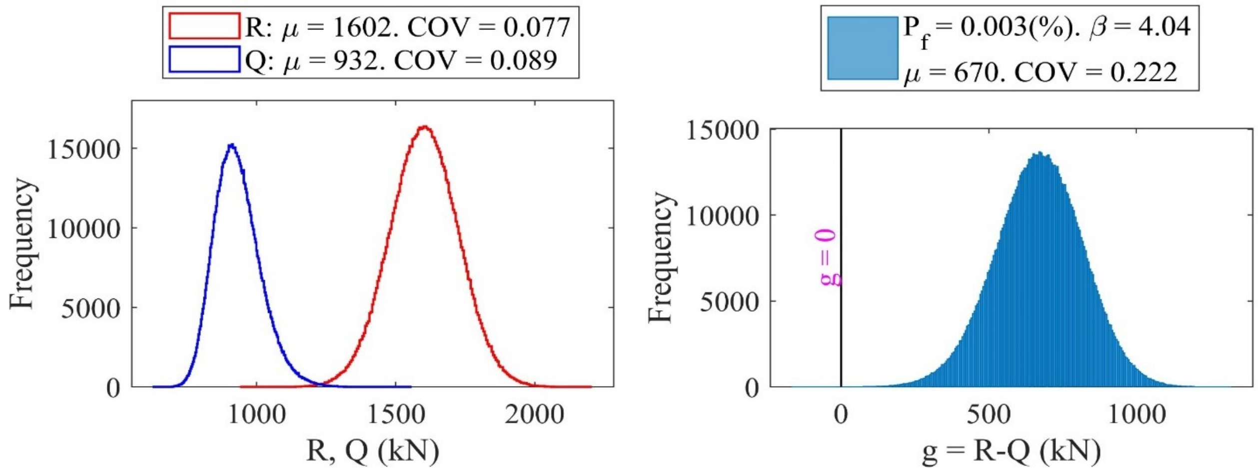

(a)

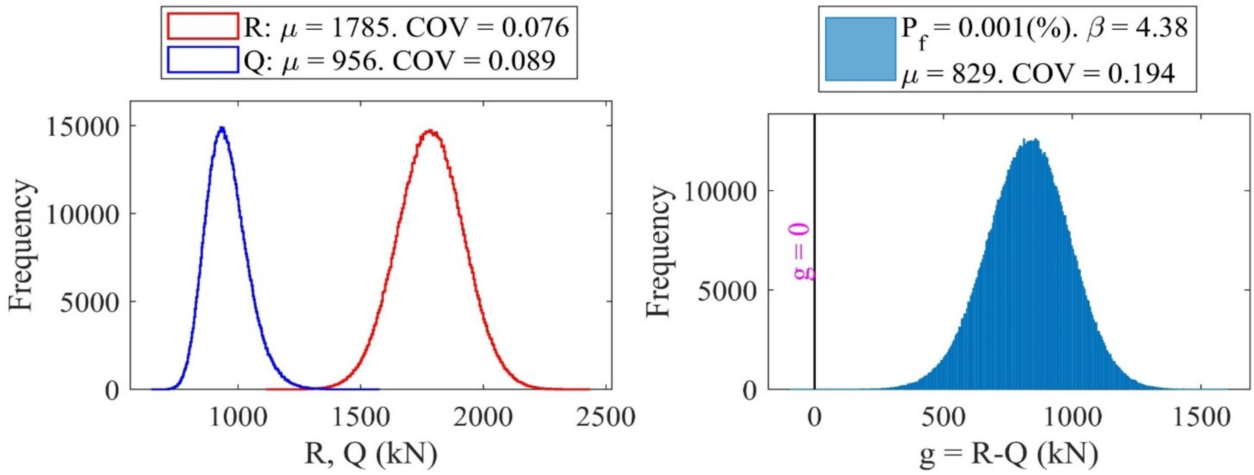

(b)

Fig. 10. Results of MCS for compression behavior: (a) Following AISC, section 200×8.8 mm; (b) Following TCVN, section 200×10 mm

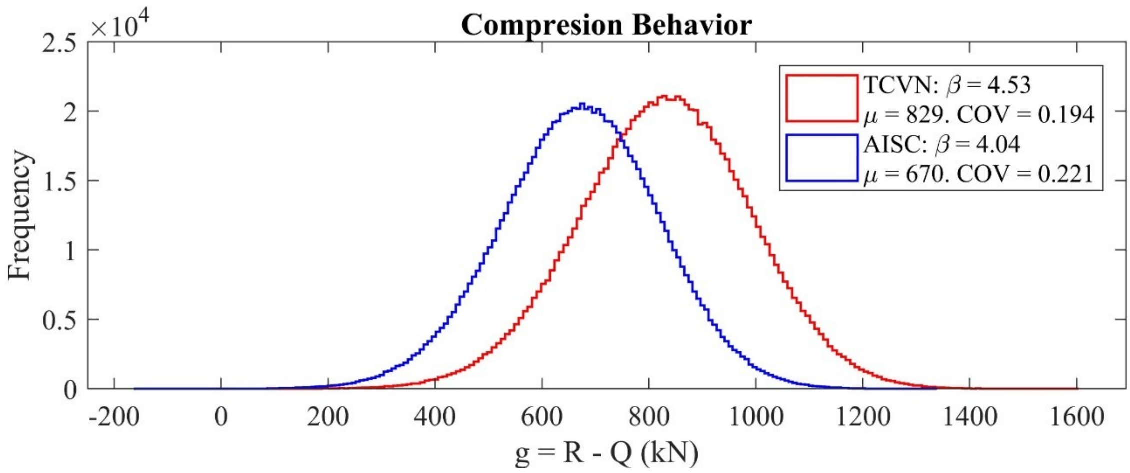

Fig. 11. Comparing results of compression behaviors

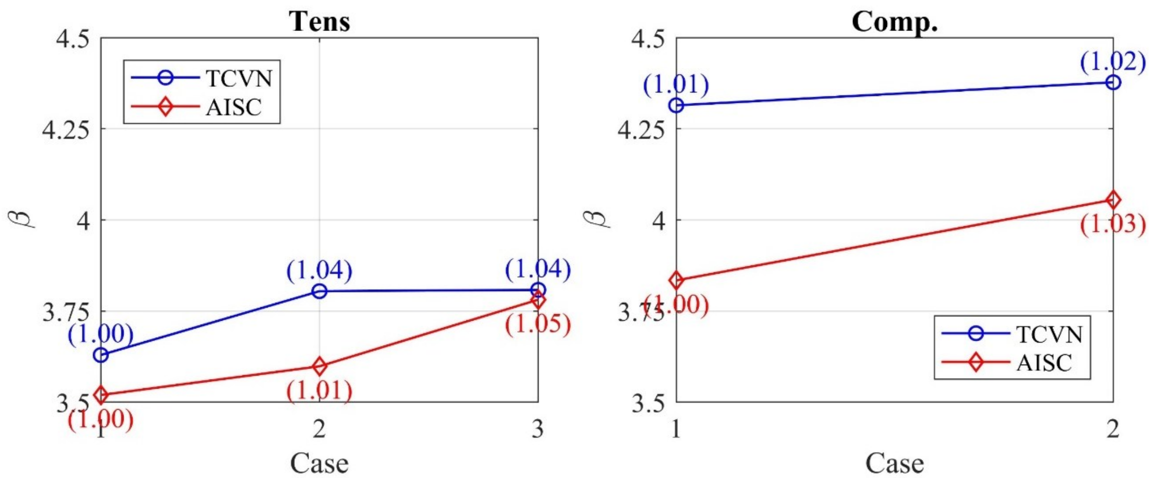

Fig. 12. Comparisons of probabilistic safety levels using the two design codes

4.3. Discussion on the factors specified in TCVN

Since closed-form solutions were employed during the development of AISC 360-16, the resulting resistance factors are lower compared to those obtained through MCS, leading to reliability indexes exceeding the target value, as shown in Fig. 12. Additionally, TCVN-based designs require larger sections compared to AISC, reflecting greater redundancy, as previously discussed. These findings suggest that to maintain a target RI of 3.0, the resistance factors in both AISC and TCVN would need recalibration.

Alternatively, if the safety level of AISC is adopted as a benchmark, only the "working condition factor" recommended in TCVN would require adjustment. It is worth noting that load factors are typically standardized across rational design codes regardless of the material, whether concrete, steel, or timber. Therefore, the load factors should remain consistent for all design materials, and recalibration should focus on resistance factors specific to the material in use. For compression behavior, an MCS-based recalibration method presented in [16] can serve as a useful reference.

The ratio of nominal resistance to load (1.67), representing the safety factor (Ω) and equivalent to a resistance factor of 0.9 for both tension and compression behaviors, is obtained from the AISC-ASD codes for an L/D ratio of 3, as detailed in Eqs. (14) and (15) below [6].

In the LRFD format of AISC:

$$\begin{aligned} \phi R_n &= 1.2D_n + 1.6L_n \\ \phi R_n &= 1.2D_n + 1.6\times 3D_n = 6D_n \\ R_n &= 6D_n/\phi \end{aligned} \tag{14}$$

In the ASD format of AISC:

$$\begin{aligned} R_n &= \Omega\left(D_n + L_n\right) \\ R_n &= \Omega\left(D_n + 3D_n\right) \\ R_n &= 4\Omega D_n \end{aligned} \tag{15}$$

From the two above equations, the safety factor Ω associated with the resistance factor ϕ can be derived as Eq. (16). That is, a safety factor of 1.67 can be used, equivalent to a resistance factor of 0.9.

$$\Omega = \frac{1.5}{\phi} \tag{16}$$

For comparison, the same equivalent safety factor for TCVN (Ω_{VN}) is also determined, as shown in Eq. (17).

$$\Omega_{VN} = \frac{1.35 + 1.5\times 3}{4}\frac{1}{\phi_{VN}} = \frac{1.46}{\phi_{VN}} \tag{17}$$

Therefore, the resistance factor ϕ_{VN} and the safety factor Ω_{VN} can be used interchangeably when applying TCVN. A minor difference in the numerators of equations (16) and (17) suggests that the load factors outlined in the two design standards are quite similar. This is further supported by Fig. 8(a), where the same section is used for both design codes (i.e., the same resistance). The load obtained from TCVN (1012 kN) is slightly higher than that from AISC (987 kN). This observation confirms that the load factors and their combination specified in TCVN are quite similar to those defined in AISC. Therefore, the significant differences in Fig. 12 for compression behaviors may be attributed to the resistance factors specified in TCVN.

In the design process of TCVN, the partial safety factor for material (γ_M), which accounts for the reliability of material strength, is applied, leading to a higher required safety factor. For instance, in tension design, an equivalent resistance factor of 0.86 (i.e., 0.95/1.1) is used, resulting in an equivalent safety factor of about 1.69 (1.46/0.86), which closely aligns with the 1.67 specified in the AISC ASD format. Since TCVN requires a slightly higher safety factor, the corresponding reliability indexes for tension members are slightly higher in TCVN, as shown in Fig. 12. This indicates that the resistance factor for tension members in TCVN is reasonably calibrated compared to AISC.

Similarly, for compression design, the equivalent safety factor of 1.78 is derived using the working condition factor (γ_c) of 0.9 specified in TCVN. This results in approximately a 7% larger safety factor, which translates into the need for 7% larger sections for compression bars when designed according to TCVN, compared to AISC (1.67). These findings explain the larger sections required for compression members in TCVN, as shown in Table 2. Consequently, the larger reliability indexes for TCVN, as presented in Fig. 12, reflect this conservative approach. Overall, these results suggest that the working condition factor specified for compression design in TCVN is conservatively set.

The above discussion emphasizes that resistance factors prescribed in the design standards for each material (e.g., concrete, steel) and the load factors defined in the “loads and actions” code must be properly aligned to maintain an appropriate safety level. For instance, if changes are made to the load factors in the loads and actions standard, corresponding adjustments should also be made to the resistance factors in the relevant design codes.

5. Conclusions

This study carries out probabilistic analyses to compare the limit state designs of a truss structure. The two limit state design codes, including AISC 360-16 and TCVN 5575-2012, are used for designing tension and compression bars of the truss structure. The MCS-based reliability analyses are then executed to evaluate the probabilistic results. Given that comparing two design codes is an ambitious objective, this study is focused on planar trusses and the ultimate limit states applied to truss members. Several conclusions are summarized as follows.

When the limit states are met, the design solutions based on both design codes exceed the target reliability index of 3.0 specified in AISC. The compression designs show more redundancies compared to the tension behaviors regardless of the design code.

The load factors and their combination in the TCVN 2737-2020 are well compared to those predefined in ASCE/SEI 7-16. A slightly greater impact of the combined loads is observed when using TCVN. This indicates that the load factors are appropriately defined in the load and action code. The variations in the design solutions can be attributed to the resistance factors specified in the steel structures design code.

The designed tension sections are relatively similar for the two design codes. Thus, it can be concluded that the factors contributing to the resistance side of the tension behaviors are relatively identical. Contrastingly, the RIs for the compression sections using TCVN 5575-2012 are significantly larger than those using AISC 360-16. Moreover, all values significantly exceed the target reliability index (RI) of 3.0 specified in AISC. The conservative designs using the current resistance factors require larger sections and more expensive costs. Therefore, the resistance factors relating to the compression design should be recalibrated to reduce the cost investment.

References

[1] T. Allen, A. Nowak, R. Bathurst. (2005). Calibration to Determine Load and Resistance Factors for Geotechnical and Structural Design. Transportation Research Circular. *Transportation Research Board of the National Academies*.

[2] T.V. Galambos. (1981). Load and Resistance Factor Design. *Engineering Journal/American Institute of Steel Construction*, 74-82.

[3] A.S. Nowak, K.R. Collins. (2012). Reliability of structures. *CRC Press*.

[4] N.S. Doan, J. Huh, V.H. Mac, D.H. Kim, K. Kwak. (2021). Calibration of Load and Resistance Factors for Breakwater Foundations under the Earthquake Loading. *Sustainability*, 13(4), 1730.

[5] American Society of Civil Engineers. (2016). ASCE Standard ASCE/SEI 7-16. Minimum Design Loads for Buildings and Other Structures.

[6] American Institute of Steel Construction. (2016). ANSI/AISC 360-16. Specification for Structural Steel Buildings, an American National Standard.

[7] L. Gardner. (2011). Designers' Guide to Eurocode 3: Design of Steel Buildings. *Inst of Civil Engineers Pub.*

[8] Ministry of Construction. (2012). TCVN 5575:2012. Steel Structures - Design standard (In Vietnamese).

[9] N.S. Doan. (2023). A study on the probabilistic safety assessment of the truss structure designed by the LRFD code. *Journal of Science and Technology in Civil Engineering (JSTCE) - HUCE*, 17(1), 111-124.

[10] H.B. Blum. (2013). Reliability-based design of truss structures by advanced analysis. Research Report R936. *School of Civil Engineering, The University of Sydney, Australia*.

[11] J.A. Packer, J. Wardenier, X.-L. Zhao, G.J. van der Vegte, Y. Kurobane. (2009). Design guide for rectangular hollow section (RHS) joints under predominantly static loading. *CIDECT*.

[12] A. Haldar, S. Mahadevan. (2000). Probability, Reliability and Statistical Methods in Engineering Design. *Wiley*.

[13] H.-B. Dinh, V.H. Mac, N.S. Doan. (2024). Comparative study on semi-probabilistic design methods to calibrate load and resistance factors for sliding stability design of caisson breakwaters. *Ocean Engineering*, 293, 116573.

[14] N.S. Doan, H.-B. Dinh. (2024). Effects of limit state data on constructing accurate surrogate models for structural reliability analyses. *Probabilistic Engineering Mechanics*, 76, 103595.

[15] N.S. Doan, V.H. Mac, H.-B. Dinh. (2024). Efficient optimization-based method for simultaneous calibration of load and resistance factors considering multiple target reliability indices. *Probabilistic Engineering Mechanics*, 78, 103695.

[16] N.S. Doan. (2024). Reliability Analysis for Tension and Compression Designs of Steel Truss Elements Using Vietnamese Codes. *Lecture Notes in Civil Engineering*, 460, 165-173.